

# Diagnostic Yield and Complication of Frameless Stereotactic Brain Biopsy

Chin Taweksomboonyat, Thara Tunthanathip, Sakchai Sae-Heng, Thakul Oearsakul

Department of Surgery,  
Division of Neurosurgery,  
Faculty of Medicine, Prince  
of Songkla University,  
Hat Yai, Songkhla 90110,  
Thailand

ABSTRACT

**Background:** With the advancement of neuronavigation technologies, frameless stereotactic brain biopsy has been developed. Previous studies proved that frameless stereotactic brain biopsy was as effective and safe as frame-based stereotactic brain biopsy. The authors aimed to find the factors associated with diagnostic yield and complication rate of frameless intracranial biopsy.

**Materials and Methods:** Frameless stereotactic brain biopsy procedures, between March 2009 and April 2017, were retrospectively reviewed from medical records including imaging studies. Using logistic regression analysis, various factors were analyzed for association with diagnostic yield and postoperative complications.

**Results:** Eighty-nine frameless stereotactic brain biopsy procedures were performed on 85 patients. The most common pathology was primary central nervous system lymphoma (43.8%), followed by low-grade glioma (15.7%), and high-grade glioma (15%), respectively. The diagnostic yield was 87.6%. Postoperative intracerebral hematoma occurred in 19% of cases; however, it was symptomatic in only one case. The size of the lesion was associated with both diagnostic yield and postoperative intracerebral hematoma complication. Lesions, larger than 3 cm in diameter, were associated with a higher rate of positive biopsy result ( $P = 0.01$ ). Lesion 3 cm or smaller than 3 cm in diameter, and intraoperative bleeding associated with a higher percentage of postoperative intracerebral hematoma complications ( $P = 0.01$ ). **Conclusions:** For frameless stereotactic brain biopsy, the size of the lesion is the essential factor determining diagnostic yield and postoperative intracerebral hematoma complication.

**KEYWORDS:** Diagnostic yield, frameless stereotactic brain biopsy, neuronavigation

## INTRODUCTION

With the advancement in neuroimaging and neuronavigation technologies, the frameless stereotactic brain biopsy has been developed. Advantages of this procedure are no need for a frame attachment, able to biopsy more than one target lesion, and no imaging artifact obscuring biopsy plan. With these advantages, the frameless brain biopsy procedure is increasing in popularity nowadays.

From previous studies, the diagnostic yield and complications are not different for the diagnosis between frame-based and frameless brain biopsies.<sup>[1-3]</sup> In details, the diagnostic yield of frameless stereotactic brain biopsy was between 88.9% and 99.7% of cases.<sup>[1,2,4,3,5-12]</sup> In literature, the age of <30 years<sup>[9]</sup> and cerebellar

lesions<sup>[3]</sup> are factors associated with nondiagnostic results whereas the numbers of biopsies associated with a higher diagnostic yield.<sup>[13]</sup>

The morbidity and mortality rates associated with this procedure were 1.0%–13.2%<sup>[1,2,14,4,6-10,12,15]</sup> and 0%–3.7%,<sup>[1,2,14,3,6-10,12,15]</sup> respectively. The rate of postoperative intracerebral hemorrhage has been reported between 2.3% and 72% of procedures.<sup>[1,3,5,7,8,12,16,15]</sup> The factors associated with this complication are serum

**Address for correspondence:** Dr. Thara Tunthanathip, Department of Surgery, Division of Neurosurgery, Faculty of Medicine, Prince of Songkla University, Hatyai, Songkhla 90110, Thailand. E-mail: tsus4@hotmail.com

This is an open access journal, and articles are distributed under the terms of the Creative Commons Attribution-NonCommercial-ShareAlike 4.0 License, which allows others to remix, tweak, and build upon the work non-commercially, as long as appropriate credit is given and the new creations are licensed under the identical terms.

For reprints contact: reprints@medknow.com

**How to cite this article:** Taweksomboonyat C, Tunthanathip T, Sae-Heng S, Oearsakul T. Diagnostic yield and complication of frameless stereotactic brain biopsy. *J Neurosci Rural Pract* 2018;10:78-84.

Access this article online	
<b>Quick Response Code:</b> 	<b>Website:</b> <a href="http://www.ruralneuropractice.com">www.ruralneuropractice.com</a>
	<b>DOI:</b> <a href="https://doi.org/10.4103/jnpr.jnpr_166_18">10.4103/jnpr.jnpr_166_18</a>

glucose levels of more than 200 mg/dL,<sup>[9]</sup> diabetic patient,<sup>[17]</sup> intraoperative bleeding complications,<sup>[10]</sup> size of biopsy needles,<sup>[16]</sup> pathological diagnosis as lymphoma,<sup>[3]</sup> and basal ganglia, thalamic, and frontotemporal location.<sup>[3,17]</sup>

The objective of this study was to identify various factors associated with diagnostic yield and postoperative intracerebral hemorrhage, in the frameless stereotactic brain biopsy procedures.

## MATERIALS AND METHODS

### Study design

Data were retrospectively collected for all patients undergoing a frameless stereotactic brain biopsy in Songklanagarind Hospital between March 2009 and April 2017. The frameless stereotactic system used in this study was the VarioGuide system (BrainLAB, Feldkirchen, Germany). Computed tomography (CT) brain scans with thin slice thickness (1-mm slice thickness) were used as preoperative navigation imaging in all procedures.

All biopsy procedures were performed under general anesthesia, the patients being positioned in either the supine or prone position, and the head was fixed with a standard three-point head clamp. A neuronavigation reference star was attached to the head clamp. Navigation was then registered by laser pointer surface registration. In some cases, fiducial registration was used for registration when in the prone position. After registration, the skin surface accuracy was finally checked. The planning of biopsy trajectory was created using this navigator system. Then, the skin was prepared using standard sterile techniques, and the stereotactic arm was attached to the head clamp and aligned to the planned trajectory.

Subsequently, a standard skin incision was verified by neuronavigation. The burr hole was created with a high-speed drill. The 3-mm diameter biopsy needle was equipped with reflectors. Then, the trajectory was created by the navigation system for biopsy. Dura was opened, and then corticotomy was performed. Sequential biopsies were performed along the planned path. Four quadrant biopsy samples were routinely taken, with an intraoperative frozen section being sent if it was available. The additional biopsies were performed when intraoperative frozen section reported as the negative result. Then, the wound was closed in standard fashion. Data about the number of biopsies, intraoperative bleeding or cerebrospinal fluid leakage complication, frozen section result, final pathological result, and postoperative complication were collected. Finally, routine postoperative CT scans of the brain

were immediately performed to confirm intracerebral pneumocephalus and postoperative complications.

### Statistical analysis

The clinical factors were analyzed using descriptive statistics and presented as proportions and mean  $\pm$  standard deviation. Therefore, using Fisher's exact test examined the relationship between the two groups for each clinical factor. Logistic regression was used to analyze the outcomes as the odds ratio (OR). In addition, variables were eliminated from the model one, at a time, based on the Akaike information criterion. Therefore, all nonsignificant variables ( $P > 0.05$ ) were removed from the multivariable analysis. The statistical analyses were performed using the R version 3.4.0 software (R Foundation, Vienna, Austria), and the R package party kit was utilized for conditional inference trees.<sup>[18,19]</sup>  $P < 0.05$  was considered as statistically significant.

## RESULTS

A total of 89 biopsies were performed on 85 patients between March 2009 and April 2017. The mean age of the patients was  $56.23 \pm 13.20$  years. There were 46 males and 39 females. Fourteen (16.5%) and 32 (37.6%) patients had underlying diabetes mellitus and hypertension, respectively. Fifty-two patients (58.4%) received preoperative dexamethasone. The most common presentation of the patients was hemiparesis (63.5%), followed by a headache (45.9%), alteration of consciousness (42.4%), and seizure (20.2%), respectively. Table 1 shows the baseline of the patients' characteristics.

The frontal lesions were the most common location in the present study (38.2%), followed by corpus callosum and periventricular region (14.6%), parietal lobe (13.5%), and thalamus (10.1%), respectively. The lesions were on the left side in 45 cases (50.6%), right side in 27 cases (30.3%), and bilaterally in 17 cases (19.1%). The lesions were heterogeneously enhanced in 39 cases (43.8%), homogeneously enhanced in 32 cases (35.9%), rim enhanced in 18 cases (20.5%), and not enhanced in three cases (3.4%). There were the butterfly and infiltrative lesions in 18 (20%) and 27 cases (30%), respectively. The mean diameter of the lesions was  $3.80 \pm 2.1$  cm. Furthermore, the mean distance between the cortex and the target of biopsy was  $3.81 \pm 1.40$  cm. Table 2 shows lesion characteristics.

Mostly, more than half of the biopsies (56%) were collected following 5–8 attempts while the number of biopsy(ies) between 1 and 4 and nine attempts were 35 and 8 in percentage, respectively. Intraoperative frozen section examination was performed in 76% of

the procedures. Frozen section examination ended with tumor diagnosis in 47/67 cases (70.1%). Moreover, the concordance between the frozen section examination and the final pathologic result was 81%.

### Diagnostic yield

As shown in Table 3, a definite pathological diagnosis was obtained in 78 of 89 procedures (87.6%). The histological diagnosis was primary central nervous system lymphoma (PCNSL) in 39 cases (43.8%), diffuse astrocytoma in 14 cases (15.7%), anaplastic astrocytoma in 8 cases (9.0%), infection in 8 cases (9.0%), glioblastoma multiforme in 5 cases (5.7%), metastasis in 2 cases (2.2%), tumor necrosis in 1 case (1.1%), and tumefactive multiple sclerosis in 1 case (1.1%). Table 3 shows the summary of pathological diagnoses.

After the procedures, postoperative CT scans of the brain were immediately performed to identify intralesional pneumocephalus to confirm if tissue sampling had appropriately been done. For example, a 51-year-old patient presented with truncal ataxia. Axial contrast enhanced-CT scan of the brain showed an enhancing 3-cm diameter mass lesion located near the fourth ventricle and frameless stereotactic biopsy was done for it. Postoperative CT scan of the brain showed intralesional pneumocephalus that indicated appropriate biopsy location as shown in Figure 1. Finally, the pathological examination was PCNSL.

**Table 1: Baseline characteristics of the patients**

Factor	n (%)
Age (years)	
<15	2 (2.4)
15-60	51 (60)
>60	32 (37.6)
Mean age of the patients (years)±SD	56.23±13.20
Sex	
Male	46 (54.1)
Underlying disease	
Diabetes mellitus	14 (16.5)
Hypertension	32 (37.6)
Coagulopathy (corrected before the operation)	3 (3.4)
Other underlying disease	35 (41.2)
Prior radiation therapy	3 (3.4)
Prior chemotherapy	5 (5.9)
Preoperative dexamethasone	52 (58.4)
Signs and symptoms	
Hemiparesis	54 (63.5)
Headache	39 (45.9)
Alteration of consciousness	36 (42.4)
Seizure	18 (20.2)
Memory deficit	5 (5.9)
Ataxia	3 (3.4)
Others	12 (13.4)

SD: Standard deviation

From univariate analysis for diagnostic yield, the diameter of the lesion was the only factor that was statistically significant correlated with diagnostic yield (Fisher's exact test,  $P = 0.02$ ) as shown in Table 4. In logistic regression analysis, the lesions of more than 3 cm in size were associated with a higher diagnostic yield compared with lesions equal to 3 cm or less in

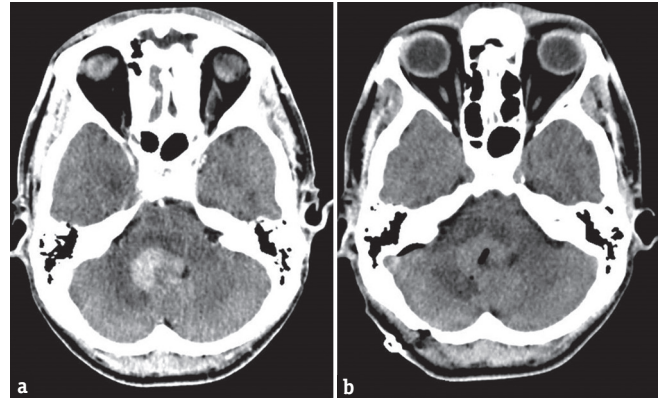


**Figure 1:** Postoperative intralesional pneumocephalus. (a) Preoperative contrast enhanced- computed tomography scan of the brain showed a 3-cm diameter enhancing periventricular fourth ventricular mass. (b) Postoperative computed tomography of the brain showed intralesional pneumocephalus without intracranial hematoma

**Table 2: Lesion characteristics**

	n (%)
Location	
Frontal	34 (38.2)
Corpus callosum/periventricular	13 (14.6)
Parietal	12 (13.5)
Thalamus	9 (10.1)
Temporal	8 (9.0)
Basal ganglion	6 (6.7)
Occipital	4 (4.5)
Cerebellum	3 (3.4)
Side	
Left	45 (50.6)
Right	27 (30.3)
Bilateral	17 (19.1)
Number of lesion	
Single	40 (45.5)
2	13 (14.8)
3	4 (4.5)
≥4	31 (35.2)
Contrast enhancement	
Rim enhancement	18 (20.5)
Homogeneous	32 (35.9)
Heterogeneous	39 (43.8)
Infiltrative lesion	27 (30.3)
Butterfly lesion	18 (20.2)
Mean distance between cortex and target (cm)±SD (range)	3.81±1.40 (1-7.5)
Mean diameter of lesion (cm)±SD (range)	3.80±2.10 (1-12.0)

SD: Standard deviation

size (OR 6.46; 95% confidence interval [CI]: 1.31–31.95,  $P = 0.01$ ). Figure 2 shows the diagnostic yield in lesion of more than and <3 cm in size according to conditional inference trees.

**Complications**

Intraoperative bleeding complications as seen from the biopsy needle during biopsy occurred in 11 operations (12.3%). From postoperative CT brain scanning, intracerebral hemorrhage occurred after 17 procedures (19.1%), in both symptomatic and asymptomatic lesions. Postoperative, new neurological deficit and death occurred in one case (1.1%). The fatal operation happened in a 70-year-old male, with a left basal ganglia lesion presented with right hemiparesis. Postoperative, massive, left basal ganglia hemorrhage was encountered, and eventually resulted in death. Table 5 shows postoperative complications associated with frameless stereotactic brain biopsy in this study.

In univariate analysis for postoperative intracerebral hemorrhage, preoperative dexamethasone ( $P = 0.035$ ), and intraoperative bleeding through the biopsy needle ( $P = 0.03$ ) as shown in Figure 3, and diameter of the lesion <3 cm ( $P = 0.007$ ) was statistically significant associated with these complications as shown in Table 6. However, multivariable analysis of logistic regression showed that intraoperative bleeding (OR: 6.42; 95%-CI: 1.55–26.63,  $P = 0.01$ ) and diameter of the lesion (OR: 6.80; 95%-CI: 1.38–33.46,  $P = 0.01$ ) were also statistically significantly correlated with this complication.

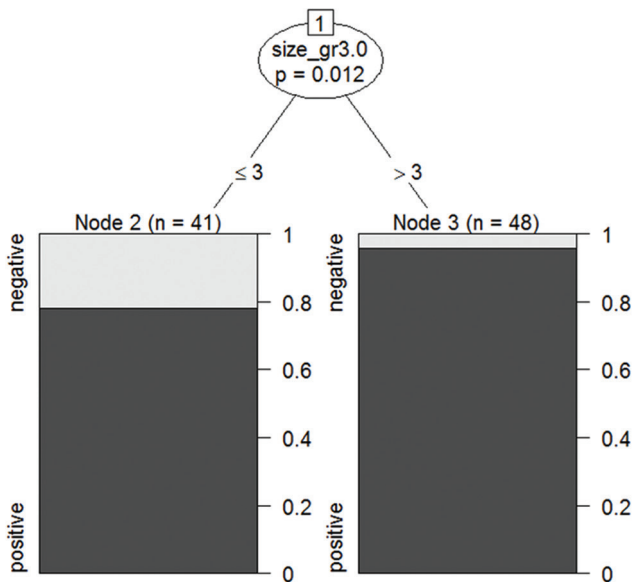


**Figure 2:** Diagnostic yield, according to the lesion size. According to conditional inference trees, the diameter of the lesion associated with diagnostic yield (node 1,  $P = 0.01$ ). There was a 78% diagnostic yield in diameter of lesions 3 cm, or less, (node 2). Conversely, lesions larger than 3 cm have a 95.8% diagnostic yield (node 3)

Figure 4 shows conditional inference trees, about factors correlated with the risk of postoperative intracerebral hemorrhage complications.

**DISCUSSION**

In the present study, the overall diagnostic yield from CT imaging was close to previous studies. In details, the diagnostic yield in this study was 87.6% comparing with 88.9%–99.7% in the literature.<sup>[1-3,5-12]</sup>

Slightly lower yields than that of the literature have occurred from CT-based registrations. However, immediate postoperative CT scanning of the brain confirmed that external intralesional air being observed in all procedures. From the literature review, the factors associated with lower diagnostic yields are the patient age of <30 years<sup>[9]</sup> and cerebellar lesion while more times of numbers of the biopsy associated with a higher diagnostic yield.<sup>[13]</sup> Moreover, the authors found that the diameter of the lesion correlated with diagnostic yield. The size of the lesions larger than 3 cm was significantly associated with higher diagnostic yield, compared with lesions of 3 cm or smaller. As to the complications, the prevalence of postoperative intracerebral hemorrhage was 2.3%–72% dependent on the definition. Several

**Table 3: Summary of pathological diagnoses**

Diagnosis	n (%)
PCNSL	39 (43.8)
Diffuse astrocytoma	14 (15.7)
Anaplastic astrocytoma	8 (9.0)
Infection	8 (9.0)
Glioblastoma multiforme	5 (5.7)
Metastasis	2 (2.2)
Tumor necrosis	1 (1.1)
Tumefactive multiple sclerosis	1 (1.1)
Nondiagnostic	11 (12.4)

PCNSL: Primary central nervous system lymphoma

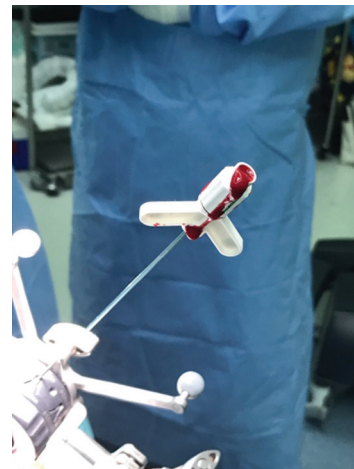


**Figure 3:** Intraoperative bleeding through the biopsy needle

studies defined only symptomatic lesions whereas some research defined hematoma as larger than 1 cm in size.<sup>[1,3,5,7,8,12,16,15]</sup> In the present study, we defined postoperative hematoma as any size of both symptomatic and asymptomatic lesions. Hence, the prevalence of postoperative intracerebral hemorrhage in this study may be higher than in some previous studies.

The factors associated with postoperative complications in previous studies are serum glucose levels more than

**Table 4: Analysis for the positive biopsy**

Factors	Diagnostic yield		P
	Positive	Negative	
Age (year)			
≤60	45 (60.8)	8 (72.7)	0.52
>60	29 (39.2)	3 (27.3)	
Sex			
Male	40 (54.1)	6 (54.5)	0.97
Female	34 (45.9)	5 (45.5)	
Prior radiotherapy*	3 (4.1)	0	1.00
Prior chemotherapy*	5 (6.8)	0	1.00
Preoperative dexamethasone injection*	47 (60.3)	5 (45.5)	0.51
Intraoperative CSF leakage*	11 (25.0)	2 (25.0)	1.00
Intraoperative hemorrhage*	11 (14.3)	0	0.34
Contrast enhancement*	75 (96.1)	11 (100)	0.91
Infiltrative lesion*	24 (30.8)	3 (27.3)	1.00
Butterfly lesion*	17 (21.8)	1 (9.1)	0.45
Multiple lesion*	39 (50.6)	9 (81.8)	0.06
Deep-seat lesion* <sup>†</sup>	25 (32.1)	3 (27.3)	1.00
Cortex - the core of lesion distance (cm)			
<4	42 (54.5)	5 (45.5)	0.57
≥4	35 (45.5)	6 (54.5)	
Mean of cortex core lesion distance±SD	3.77±1.42	3.9±1.5	0.74
Attempt of biopsy			
≤4	27 (39.1)	1 (9.1)	0.08
>4	412 (60.9)	10 (90.9)	
Diameter (cm)			
≤3	32 (41.0)	9 (81.8)	0.02
>3	46 (59.0)	2 (18.2)	

\*Data show only “yes group” while reference groups (no group) are hidden, <sup>†</sup>Deep-seated lesion consists of corpus callosum, thalamic, and basal ganglion lesion. CSF: Cerebrospinal fluid, SD: Standard deviation

**Table 5: Postoperative complications**

Complications	n (%)
Intraoperative Hemorrhage	11 (12.3)
Postoperative Hematoma	17 (19.1)
New neurological deficit	1 (1.1)
Biopsy-related mortality	1 (1.1)

200 mg/dL,<sup>[9]</sup> diabetic patients,<sup>[17]</sup> intraoperative bleeding complications,<sup>[9]</sup> size of biopsy needle,<sup>[16]</sup> pathological diagnosis as lymphoma,<sup>[3]</sup> basal ganglia, thalamic, and frontotemporal locations.<sup>[3,17]</sup> In this study, we found that intraoperative bleeding complications and lesions 3 cm or smaller were correlated with a higher incidence of postoperative intracerebral hemorrhage. Moreover, the morbidity and mortality rates of biopsy procedures were reported between 1.0%–13.2%<sup>[1,2,14,3,6-10,12,15]</sup> and 0%–3.7%,<sup>[1,2,14,3,6-10,12,15]</sup> respectively. Equally, the morbidity and mortality rates in the present study were both 1.1%.

Limitations of the present study should be acknowledged. First, this retrospective study design may lead to bias and cannot control confounding factors. However, we used multivariable analysis to correct these limitations. Second, our institute used CT-based registration for the navigation system, which requires further studies to compare the efficacy of diagnostic yield between CT-based and magnetic resonance image-based registration.

Strengths of the present study are that, to the author’s knowledge, this is the first study that identified the lesion size as a novel factor associated with diagnostic yield and postoperative intracerebral hemorrhage. In addition, intraoperative bleeding through the biopsy needle was vital to predict postoperative intracerebral hematoma.

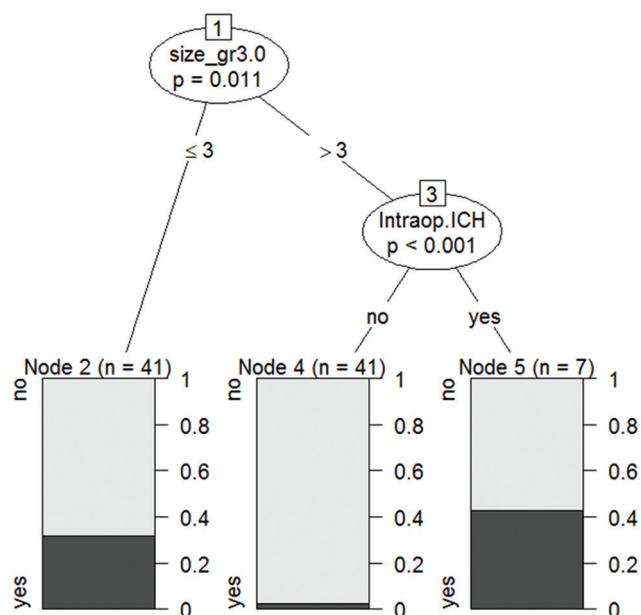


**Figure 4:** Risk of postoperative intracerebral hemorrhage. According to conditional inference trees, size of the lesion was associated with bleeding complication (node 1,  $P = 0.01$ ). The small lesions (3 cm and less in diameter) were 78% of postoperative bleeding (node 2) while lesion larger than 3 cm without intraoperative bleeding have complication of about 2.4 (node 4). Lesions larger than 3 cm, with intraoperative bleeding, were observed in 42.9%. Intraoperative bleeding was a statistically significant indicator to predict postoperative complications (node 5,  $P < 0.001$ )

**Table 6: Univariate analysis for postoperative intracerebral hematoma**

Factors	Postop ICH		P
	No (%)	Yes (%)	
Age (year)			
≤60	45 (65.2)	8 (50)	0.26
>60	24 (34.8)	8 (50)	
Sex			
Male	35 (50.7)	11 (68.8)	0.26
Female	34 (49.3)	5 (31.2)	
DM*	9 (13.2)	5 (31.2)	0.12
Hypertension*	23 (33.8)	9 (56.2)	0.15
Preoperative coagulopathy*	2 (2.9)	1 (6.2)	0.47
Prior radiotherapy*	3 (4.4)	0	1.00
Prior chemotherapy*	5 (7.4)	0	0.57
Preoperative dexamethasone injection*	45 (63.4)	6 (35.3)	0.035
Intraoperative CSF leakage*	9 (24.3)	4 (28.6)	0.75
Intraoperative hemorrhage*	6 (8.6)	5 (29.4)	0.03
Contrast enhancement *	68 (95.7)	17 (100)	0.77
Infiltrative lesion*	25 (35.2)	2 (11.8)	0.08
Deep-seat lesion*,†	21 (29.6)	7 (41.2)	0.31
Multiple lesion*	37 (52.9)	11 (64.7)	0.37
PCNSL*	30 (48.4)	9 (60.0)	0.56
Glioma*	22 (35.5)	4 (26.7)	0.76
Cortex core lesion distance (cm)			
≤3	25 (35.2)	7 (41.2)	0.78
>3	46 (64.8)	10 (58.8)	
Attempt of biopsy			
≤4	24 (38.1)	4 (25.0)	0.39
>4	39 (61.9)	12 (75.0)	
The diameter of the tumor (cm)			
≤3	28 (39.4)	13 (76.5)	0.007
>3	43 (60.6)	4 (23.5)	

\*Data show only “yes group” while reference groups (no group) are hidden, †Deep-seated lesion consists of corpus callosum, thalamic, and basal ganglion lesion. CSF: Cerebrospinal fluid, DM: Diabetes mellitus, ICH: Intracerebral hemorrhage, PCNSL: Primary central nervous system lymphoma

These results from the present study can be applied in real-world clinical practice.

## CONCLUSION

In summary, the diameter of the lesion more than 3 cm is essential in predicting diagnostic yield, while small lesions were associated with the postoperative hematoma.

## Financial support and sponsorship

Nil.

## Conflicts of interest

There are no conflicts of interest.

## REFERENCES

- Woodworth GF, McGirt MJ, Samdani A, Garonik I, Olivi A, Weingart JD, *et al.* Frameless image-guided stereotactic brain biopsy procedure: Diagnostic yield, surgical morbidity, and comparison with the frame-based technique. *J Neurosurg* 2006;104:233-7.
- Smith JS, Quiñones-Hinojosa A, Barbaro NM, McDermott MW. Frame-based stereotactic biopsy remains an important diagnostic tool with distinct advantages over frameless stereotactic biopsy. *J Neurooncol* 2005;73:173-9.
- Dammers R, Haitsma IK, Schouten JW, Kros JM, Avezaat CJ, Vincent AJ. Safety and efficacy of frameless and frame-based intracranial biopsy techniques. *Acta Neurochir (Wien)* 2008;150:23-9.
- Nishihara M, Takeda N, Harada T, Kidoguchi K, Tatsumi S, Tanaka K, *et al.* Diagnostic yield and morbidity by neuronavigation-guided frameless stereotactic biopsy using magnetic resonance imaging and by frame-based computed tomography-guided stereotactic biopsy. *Surg Neurol Int* 2014;5:S421-6.
- Fрати A, Pichiерri A, Bastianello S, Raco A, Santoro A, Esposito V, *et al.* Frameless stereotactic cerebral biopsy: Our experience in 296 cases. *Stereotact Funct Neurosurg* 2011;89:234-45.
- Shooman D, Belli A, Grundy PL. Image-guided frameless stereotactic biopsy without intraoperative neuropathological examination. *J Neurosurg* 2010;113:170-8.
- Barnett GH, Miller DW, Weisenberger J. Frameless stereotaxy with scalp-applied fiducial markers for brain biopsy procedures: Experience in 218 cases. *J Neurosurg* 1999;91:569-76.
- Gempt J, Buchmann N, Ryang YM, Krieg S, Kreutzer J, Meyer B, *et al.* Frameless image-guided stereotaxy with real-time visual feedback for brain biopsy. *Acta Neurochir (Wien)* 2012;154:1663-7.
- Khatab S, Spliet W, Woerdeman PA. Frameless image-guided stereotactic brain biopsies: Emphasis on diagnostic yield. *Acta Neurochir (Wien)* 2014;156:1441-50.
- Dammers R, Schouten JW, Haitsma IK, Vincent AJ, Kros JM, Dirven CM, *et al.* Towards improving the safety and diagnostic yield of stereotactic biopsy in a single centre. *Acta Neurochir (Wien)* 2010;152:1915-21.
- Lu Y, Yeung C, Radmanesh A, Wiemann R, Black PM, Golby AJ, *et al.* Comparative effectiveness of frame-based, frameless, and intraoperative magnetic resonance imaging-guided brain biopsy techniques. *World Neurosurg* 2015;83:261-8.
- Air EL, Leach JL, Warnick RE, McPherson CM. Comparing the risks of frameless stereotactic biopsy in eloquent and noneloquent regions of the brain: A retrospective review of 284 cases. *J Neurosurg* 2009;111:820-4.
- Jain D, Sharma MC, Sarkar C, Deb P, Gupta D, Mahapatra AK, *et al.* Correlation of diagnostic yield of stereotactic brain biopsy with number of biopsy bits and site of the lesion. *Brain Tumor Pathol* 2006;23:71-5.
- Dorward NL, Paleologos TS, Alberti O, Thomas DG. The advantages of frameless stereotactic biopsy over frame-based biopsy. *Br J Neurosurg* 2002;16:110-8.
- Ringel F, Ingerl D, Ott S, Meyer B. VarioGuide: A new frameless image-guided stereotactic system – Accuracy study and clinical assessment. *Neurosurgery* 2009;64:365-71.
- Yuen J, Zhu CX, Chan DT, Ng RY, Nia W, Poon WS, *et al.* A sequential comparison on the risk of haemorrhage with different sizes of biopsy needles for stereotactic brain biopsy. *Stereotact Funct Neurosurg* 2014;92:160-9.

17. McGirt MJ, Woodworth GF, Coon AL, Frazier JM, Amundson E, Garonzik I, *et al.* Independent predictors of morbidity after image-guided stereotactic brain biopsy: A risk assessment of 270 cases. *J Neurosurg* 2005;102:897-901.
18. Horthorn T, Zeileis A. Toolkit for Recursive Partitioning. Austria: The R Foundation; 2016. Available from: <http://www.cran.r-project.org/web/packages/partykit/index.html>. [Last accessed on 2017 Jan 09].
19. Horthorn T, Hornik K, Zeileis A. Party: A Laboratory for Recursive Partitioning. Austria: The R Foundation; 1999. Available from: <http://www.cran.r-project.org/web/packages/party/vignettes/party.pdf>. [Last accessed on 2017 Jan 10].